Cell, Vol. 87, 205–216, October 18, 1996, Copyright ©1996 by Cell Press

MEX-3 Is a KH Domain Protein That Regulates Blastomere Identity in Early C. elegans Embryos

Bruce W. Draper,*† Craig C. Mello,*‖
Bruce Bowerman,*# Jeff Hardin,‡
and James R. Priess,*†§
*Department of Basic Sciences
Fred Hutchinson Cancer Research Center
Seattle, Washington 98109
†Zoology Department
University of Washington
Seattle, Washington 98195
‡Department of Zoology
University of Wisconsin
Madison, Wisconsin 53706
§Howard Hughes Medical Institute

Summary

After the first division of the C. elegans embryo, the posterior blastomere can produce numerous muscles while the anterior blastomere cannot. We show here that maternal-effect lethal mutations in the gene *mex-3* cause descendants of the anterior blastomere to produce muscles by a pattern of development similar to that of a descendant of the wild-type posterior blastomere. *mex-3* encodes a probable RNA-binding protein that is distributed unequally in early embryos and that is a component of germline-specific granules called P granules. We propose that MEX-3 contributes to anterior–posterior asymmetry by regulating one or more mRNAs involved in specifying the fate of the posterior blastomere.

Introduction

The early cells, or blastomeres, in many animal embryos undergo distinct patterns of differentiation when isolated and cultured separately. For example, if the first two blastomeres of the C. elegans embryo are separated, the anterior blastomere, AB, does not produce muscles while the posterior blastomere, P_1, produces numerous muscles (Laufer et al., 1980; Priess and Thomson, 1987). Since these differences do not require interactions between the blastomeres, they have been described as being cell-intrinsic, or cell-autonomous, and are thought to result from the action of factors that are distributed unequally in the early embryo.

Recent studies have provided molecular evidence for anterior–posterior asymmetry in the C. elegans embryo prior to the first cell division. The PAR-3 protein is localized to the anterior cortex of the 1-cell stage embryo, and the PAR-1 protein is localized in a reciprocal pattern to the posterior cortex (Etemad-Moghadam et al., 1995; Guo and Kemphues, 1995). Genetic studies indicate that PAR-3 and PAR-1 are required for many of the differences between the AB and P_1 blastomeres after the first cleavage of the embryo (Kemphues et al., 1988; Kirby et al., 1990), but it is not yet understood how the cortically localized PAR proteins result in anterior–posterior differences in gene expression.

Two nuclear proteins have been identified that may directly regulate gene expression and that are present at high levels in the P_1 blastomere, but at low or undetectable levels in the AB blastomere. SKN-1 is a transcription factor required for the proper development of one of the P_1 daughters (Bowerman et al., 1992, 1993; Blackwell et al., 1994), and PIE-1 is a novel protein required for the development of the other P_1 daughter (Mello et al., 1992, 1996). If SKN-1 and PIE-1 were the only regulators that made P_1 different from AB, the P_1 and AB blastomeres should have identical patterns of development in *skn-1;pie-1* double mutants. Instead, the P_1 blastomere in a *skn-1;pie-1* double mutant embryo produces numerous muscles while the AB blastomere does not (Mello et al., 1992). Thus there must be at least one additional anterior–posterior asymmetry in the C. elegans embryo that prevents AB from producing muscles.

In this paper we show that mutations in the *mex-3* gene result in the AB blastomere producing numerous muscles. Previous studies have shown that mutations in the *mex-1* gene can also cause AB to produce muscles (Mello et al., 1992; Schnabel et al., 1996). In *mex-1* mutants, this defect appears to result from inappropriate, anterior expression of the SKN-1 transcription factor (Mello et al., 1992; Bowerman et al., 1993). In contrast, we show here that *mex-3* mutants do not appear to misexpress SKN-1 in AB and that the AB blastomere in a *mex-3* mutant does not require *skn-1(+)* activity to produce muscles. We therefore conclude that *mex-3(+)* functions in a second asymmetry that normally prevents AB from producing muscles. We show that the *mex-3* gene encodes a probable RNA-binding protein, suggesting that *mex-3(+)* influences anterior–posterior differences in muscle development by controlling the expression of one or more RNAs in the early embryo.

Results

The *mex-3* Locus

In wild-type embryogenesis almost all of the body-wall muscles are produced by descendants of the P_1 blastomere (Figure 1). In genetic screens for maternal-effect lethal mutations, we identified two classes of mutants with markedly abnormal patterns of body-wall muscles. In wild-type embryos, body-wall muscles are located inside the body and are covered by hypodermal cells (Sulston et al., 1983). In both classes of mutants, morphogenesis was severely abnormal and body-wall muscles were present on the external surface of the embryo. The first class of mutants corresponded to new alleles of the *par* genes. The *par* genes have been described previously and appear to function in establishing the

‖Present address: Cancer Center, University of Massachusetts, Worcester, Massachusetts 01605.
#Present address: Institute of Molecular Biology, University of Oregon, Eugene, Oregon 97403.

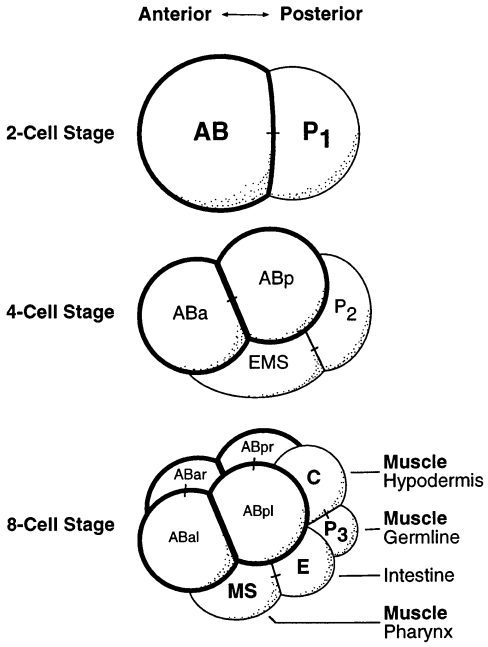

Figure 1. Cleavage Patterns and Fates of Early Blastomeres

Schematic drawings of early embryos; anterior is left. AB and its descendants are outlined in bold. Tissues made by the P_1 granddaughters C, P_3, E, and MS are listed. For a detailed description of the C. elegans lineage see Sulston et al. (1983).

initial anterior–posterior polarity of the embryo; the early blastomeres in *par* mutants have abnormal sizes and cleavage patterns (Kemphues et al., 1988; Kirby et al., 1990; Morton et al., 1992; Cheng et al., 1995). The second class of 16 mutants had early blastomeres that appeared relatively normal in size and cleavage pattern. Six of these mutants had mutations in the *mex-1* gene, which has been described previously (Mello et al., 1992; Schnabel et al., 1996). The remaining 10 mutants define a new gene that we call *mex-3* (*mex* = *m*uscle *ex*cess).

All *mex-3* alleles result in fully penetrant, recessive, strict maternal-effect embryonic lethality, and all alleles result in similar terminal phenotypes (see Experimental Procedures for genetic tests). The results described in this paper are from an analysis of the allele *mex-3(zu155)* unless indicated otherwise; embryos from *mex-3(zu155)* mothers do not contain any detectable MEX-3 protein or *mex-3* mRNA (see below). For simplicity, we refer to embryos from homozygous mutant mothers as *mex-3* mutants. We refer to body-wall muscles as simply "muscles," and all other types of muscle by specific names, such as pharyngeal muscle.

mex-3 Mutations Cause AB to Produce Muscles

Terminal stage *mex-3* mutant embryos appear to lack some of the tissues normally produced by the AB blastomere, including neurons and the anterior half of the pharynx (Figure 2). In the regions where these tissues form in wild-type embryos, *mex-3* mutants instead have numerous muscles and hypodermal cells (Figure 2C). We tested whether the AB blastomere was the source of these extra muscles by using a laser microbeam to kill the P_1 blastomere, thus allowing only AB to develop. A wild-type AB blastomere produced neurons and hypodermal cells in control experiments, but either few or no muscles (Figure 3A; Table 1). In contrast, a *mex-3* mutant AB blastomere produced numerous muscles and hypodermal cells (compare Figures 3C and 3A; Table 1).

Previous studies have shown that *mex-1* mutations cause the AB blastomere to produce muscles, apparently due to the inappropriate expression of the SKN-1 transcription factor in AB (Mello et al., 1992; Bowerman et al., 1993). We therefore asked if SKN-1 protein accumulated inappropriately in AB descendants in *mex-3* mutants, and whether *skn-1(+)* activity was required for these AB descendants to produce muscles. We stained *mex-3* mutant embryos with antibodies specific for SKN-1 protein and found that these embryos had a wild-type distribution of SKN-1 (data not shown). We next constructed and examined *mex-3;skn-1* double mutants using *skn-1(zu67)*, a nonsense mutation that should result in a nonfunctional partial protein lacking the SKN-1 DNA-binding domain (Bowerman et al., 1993; Blackwell et al., 1994; C. Schubert, B. B., and J. R. P., unpublished data). We found that AB produced numerous muscle cells in *mex-3;skn-1* double mutant embryos (Figure 3E), indicating that the AB-derived muscles in *mex-3* single

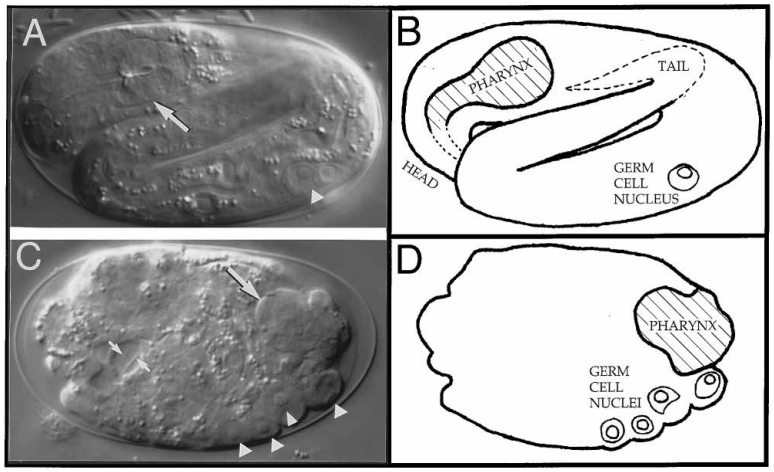

Figure 2. Wild-Type and *mex-3* Embryos

Photomicrographs of (A) wild-type and (C) *mex-3(zu155)* embryos taken 14 hr after first cleavage at 20°C. (B) and (D) are schematic diagrams of embryos shown in (A) and (C), respectively. The wild-type embryo has elongated into a worm and is near hatching. The *mex-3* embryo has not undergone body morphogenesis and contains cavities filled with muscle processes (small arrows). Pharyngeal tissue (large arrows) is indicated in both embryos. Wild-type embryos contain two germ cells; these are large cells (arrowhead in [A]; second germ cell is not visible). *mex-3* embryos often have 3–6 cells that morphologically resemble germ cells; the *mex-3* embryo shown has four such cells (arrowheads in [C]). Eggs are approximately 50 μm in length.

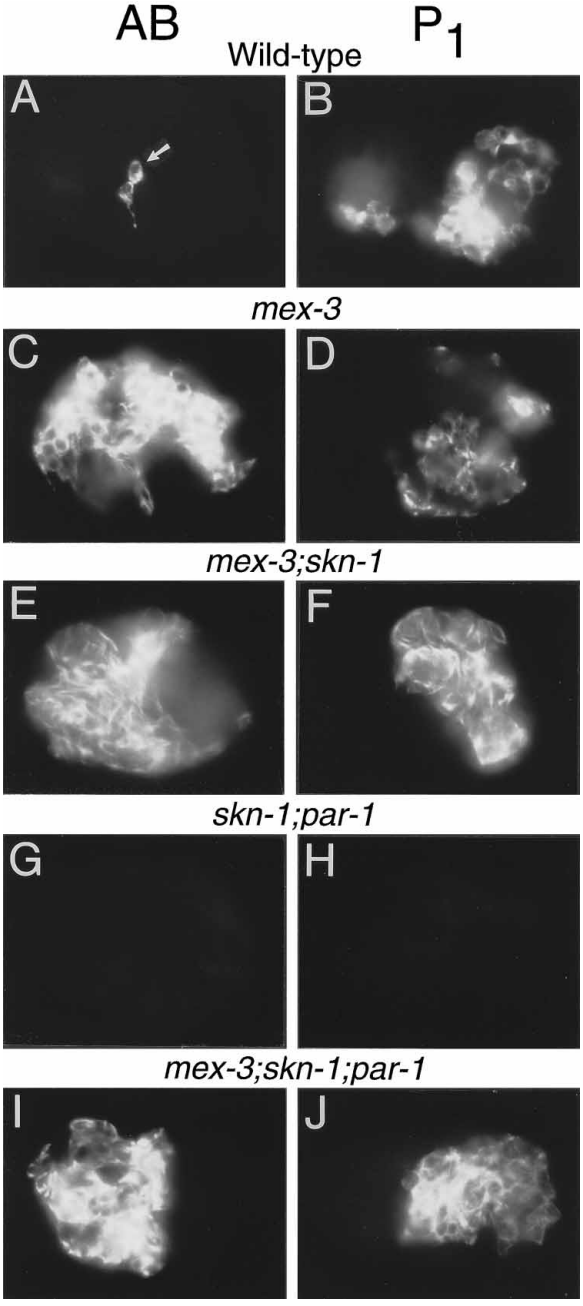

Figure 3. Muscles Production from AB or P_1

Immunofluorescence micrographs of muscle cells in partial embryos derived from either the AB (left column), or P_1 (right column) blastomere after the sister blastomere was killed; staining is with mAb 5.6 (Miller et al., 1983). A wild-type AB blastomere produces few or no muscle cells (A, arrow points to the cell body of one of two muscles), while a wild-type P_1 blastomere (B) produces numerous muscles. Both the AB and P_1 blastomeres from *mex-3* (C and D), *mex-3;skn-1* (E and F), or *mex-3;par-1;skn-1* (I and J) mutant embryos produce numerous muscles. Muscles are not produced by most *skn-1;par-1* mutant AB blastomeres (G; n = 7/8), or any *skn-1;par-1* mutant P_1 blastomeres (H; n = 11/11). Of nonoperated *skn-1;par-1* mutant embryos, 80% do not produce muscles (Bowerman et al., 1993). Mutant alleles used in these experiments were: *mex-3(zu155)*, *skn-1(zu67)*, and *par-1(e2012)*.

Table 1. Development of the AB Blastomere

	Pharynx	Valve Cells	Neurons[a]	> 4 Muscles[b]
Wild-type	10/10	16/16	32/32	0/32
mex-3	0/6	0/23	0/19	19/19
mex-3; skn-1	ND	ND	0/13	13/13
mex-3; skn-1; par-1	ND	ND	4/7	8/8

AB normally produces pharyngeal cells and intestinal valve cells (valve cells) through cell–cell interactions with P_1 descendants. P_1 descendants were allowed to interact with AB descendants, then killed with a laser microbeam so that only AB development could be scored (see Experimental Procedures). The mutant alleles used in these experiments were *mex-3(zu155), skn-1(zu67)* and *par-1(e2012)*. In addition to the cell types listed above, *mex-3* mutant AB blastomeres also produce hypodermis (56/56).

[a] Partial embryos were scored positive for neurons only if they produced a large cluster of neurons. In these experiments, *mex-3* mutant AB blastomeres produced few, if any, neurons.

[b] Embryos were scored positively for muscle if they produced more than the 2–4 muscles that a wild-type AB normally produces in these experiments. For an example of staining in wild-type embryos, see Figure 3A, and for example of staining in *mex-3(zu155)*, see Figure 3C. ND, not determined.

mutants (Figure 3C) do not result from *skn-1(+)* activity (Table 1).

AB Descendants Adopt C-like Fates in *mex-3* Mutants

In wild-type embryogenesis the fates of many AB descendants are determined through a series of cell–cell interactions (for review, see Schnabel, 1996). In the presence of the appropriate signaling cells, a wild-type AB blastomere can produce pharyngeal tissue and valve cells; these tissues are not produced when the signaling cells, or the precursors to the signaling cells, are killed with a laser microbeam. We found that the *mex-3* mutant AB blastomeres did not produce pharyngeal tissue or valve cells in the presence of the signaling cells (Table 1). In all experiments, these AB descendants appeared to produce only muscles and hypodermal cells (Tables 1 and 2), as do AB descendants when cell signaling is prevented by killing P_1 (Figure 3C). The interactions that determine the fates of wild-type AB descendants involve a receptor, GLP-1, that is expressed on AB descendants and a ligand, APX-1, that is expressed on one of the signaling cells (Evans et al., 1994; Mickey et al., 1996). We stained *mex-3* mutants with antibodies against either GLP-1 or APX-1 and found that these proteins appeared to have wild-type expression patterns (data not shown). Thus the fates of AB descendants in *mex-3* mutants do not appear to be influenced by cell–cell interactions, although the receptor and one of the known ligands are expressed in the correct cells at the correct time.

The development of individual AB descendants was analyzed in living *mex-3* mutant embryos with the light microscope to determine the source of the hypodermal cells and muscles. We found that each of the AB great-granddaughters examined had a pattern of cleavage and differentiation similar to that of a wild-type P_1 descendant, called C (Figure 4 and Table 3). In wild-type embryos, the daughters of C (such as Ca shown in Figure

Table 2. Development of AB and P_1 Granddaughters

	Wild-type		*mex-3(zu155)*	
Blastomere	Muscles	Neurons	Muscles	Neurons
AB Granddaughters				
ABal	0/12	12/12	11/11	0/11
ABar	0/8	8/8	13/13	0/13
ABpl	0/16	16/16	17/17	0/17
ABpr	0/19	19/19	17/17	0/17
P_1 Granddaughters				
C	7/7	ND	11/11	ND
P_3	17/17	ND	6/14	ND
E	0/10	ND	0/8	ND
MS	10/10	ND	16/16	ND

After killing all other blastomeres with a laser microbeam, the blastomere listed was allowed to develop for 20 hr at 15°C, then fixed and immunostained to identify muscles and neurons (see Experimental Procedures). In all experiments on wild-type or *mex-3* mutant embryos, AB descendants also produced hypodermis. Scoring for muscle was as described in Table 1. In addition to the cell types listed above, the P_1 granddaughters produce the following cell types: C produced hypodermal cells (20/20), P_3 produced germ cells (18/18), E produced intestinal cells (8/8) and MS produced pharyngeal cells (16/16). ND, not determined.

4) divide into posterior daughters that are muscle precursors and anterior daughters that are predominantly hypodermal precursors. In *mex-3* mutants, the daughters of the AB great-granddaughters (such as ABalpa in Figure 4) divide into posterior daughters that produce muscle cells and anterior daughters that produce predominantly hypodermal cells. These results suggest that in *mex-3* mutant embryos, the eight AB great-granddaughters are adopting a pattern of development similar to a wild-type C-blastomere. Thus a pattern of development that normally occurs in the posterior of a wild-type embryo occurs in the anterior of *mex-3* mutant embryos.

mex-3 Encodes a Protein with KH Domains

To begin a molecular analysis of the *mex-3* locus we searched for spontaneous alleles of *mex-3* in a mutator strain with mobile transposons (Mori et al., 1988). Four spontaneous *mex-3* alleles were isolated in this screen, and a novel Tc1 transposon insertion that comapped with the *mex-3(zu166::Tc1)* mutation was identified (see Experimental Procedures). The genomic DNA flanking the transposon insertion was isolated and used as a probe to identify potential *mex-3* genomic and cDNA clones. Sequence analysis revealed a single gene that spans about 7 kb with the inferred intron/exon boundaries shown in Figure 5A. The Tc1 associated with the *mex-3(zu166::Tc1)* mutation is inserted in the third exon of this gene (Figure 5A). We found that five other *mex-3* mutant alleles have DNA polymorphisms associated with this locus: *zu176::Tc1* is a complex DNA rearrangement associated with a novel Tc1 insertion in the third exon (data not shown), *or20* is a 419 bp deletion that removes the first 92 bp of coding sequence (Figure 5A), and *zu205*, *zu208*, and *or6* are missense mutations (Figure 5D). In addition, injection of antisense *mex-3* RNA into the gonad of wild-type hermaphrodites produces embryos that have a *mex-3* phenotype (data not shown). These results indicate that we have identified the *mex-3* gene.

The *mex-3* cDNA sequence contains an SL1 trans-spliced leader sequence (Krause and Hirsh, 1987) at its 5′ end and has a single open reading frame of 415 amino acids (Figure 5B). The predicted MEX-3 protein contains two 70–amino acid regions that are 40% identical to each other (shaded residues in Figure 5B). Database searches indicate that these repeated sequences correspond to a previously identified protein motif called a KH domain (Figure 5C) (Siomi et al., 1993). KH domains were first described in the hnRNP K protein, a pre-mRNA-binding protein (Siomi et al., 1993). The KH domain has now been found in several proteins that are known to interact with RNA, and there is evidence that this motif constitutes a single-stranded RNA binding domain (Ito et al., 1994; Leffers et al., 1995; Liu and Hanna, 1995; Urlaub et al., 1995). Mutations in several KH domain–containing proteins lead to developmental defects. These include the human fragile-X and mental retardation protein, FMR1 (Ashley et al., 1993; Gibson et al., 1993), the Drosophila protein BICAUDAL-C (Mahone et al., 1995), and the C. elegans protein GLD-1 (Jones and Schedl, 1995). A search of the nucleotide databases identified several human embryonic expressed sequence tags (ESTs) with extensive similarity to *mex-3*. The human sequences appear to represent a

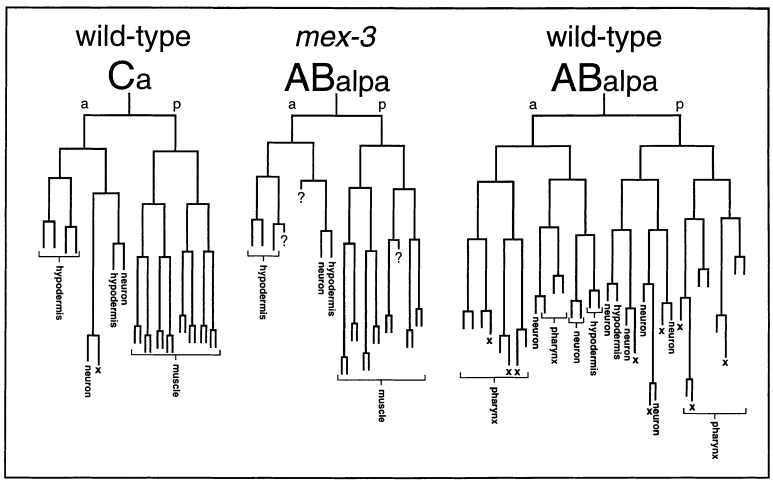

Figure 4. Cell Lineages in *mex-3 (zu155)* and Wild-Type Embryos

Lineage diagrams of ABalpa, the anterior daughter of an AB great-granddaughter, and Ca, the anterior daughter of the C blastomere (wild-type lineages described in Sulston et al., 1983). Branches represent cell division, with anterior daughters left and posterior daughters right. Lengths of vertical lines represent time. Cell fates are listed; "x" indicates cell death, "?" indicates fate could not be determined. The Ca blastomere in *mex-3* mutant embryos appears to have a wild-type pattern of development (data not shown). Additional cells examined are shown in Table 3.

Table 3. Cell Differentiation in *mex-3* Mutant Embryos

Cell Name	Fate in Wild-Type	Fate in *mex-3*	C equivalent
ABala			
paapp	2 neur, 1 death	1 hyp	1 hyp
pappa	2 neur, 1 death	1 hyp	1 hyp
ABalp			
aaaa	3 neur, 1 death	2 hyp	2 hyp
aaapa	1 neur, 1 death	1 hyp	1 hyp
aapp	2 hyp, 2 neur	1 hyp, 1 neur	1 hyp, 1 neur
apaa	2 neur, 1 hyp, 1 death	4 mus	4 mus
apap	3 neur, 2 death	4 mus	4 mus
appaa	1 neur, 2 death	2 mus	2 mus
appp	3neur, 1 death	4 mus	4 mus
paaa	2 neur, 1 death	2 hyp	2 hyp
ppppp	3 neur, 1 death	2 mus	2 mus
ABara			
paaaa	2 phar	1 hyp	1 hyp
paap	3 phar, 1 death	2 hyp	2 hyp
pappa	1 phar, 1 death	1 hyp	1 hyp
ppaaaa	1 neur	1 mus	1 mus
ppapp	2 neur	2 mus	2 mus
pppaaa	1 neur	1 mus	1 mus
ppppa	2 neur	2 mus	2 mus
ppppp	2 neur, 1 death	2 mus	2 mus
ABpla			
aapp	2 hyp	1 hyp, 1 neur	1 hyp, 1 neur
apaaa	1 hyp, 1 neur	2 mus	2 mus
ABplp			
aaaa	3 neur, 1 exc. duct	2 hyp	2 hyp
aaap	4 neur, 1 death	2 hyp	2 hyp
aappp	2 neur, 1 death	1 hyp	1 hyp
paaa	2 neur, 2 deaths	2 hyp	2 hyp
papa	5 neur	2 hyp	2 hyp

The name of each cell analyzed is listed in the first column, its fate in wild-type embryogenesis is listed in the second column, and its fate in a *mex-3* mutant is listed in the third column. The fourth column shows the fate of the lineally equivalent descendant of a wild-type C blastomere. For example, if **ABara** in a *mex-3* mutant were developing similar to a wild-type **C** blastomere, than **ABara**ppppp would be the lineal homolog of **C**ppppp. In *mex-3* mutants, **ABara**ppppp produces two muscle cells, as does **C**ppppp in wild-type embryos. In contrast, a wild-type **ABara**ppppp produces two neurons and a programmed cell death. In three cases, the axes of a cell division being followed was not anterior–posterior, but was instead left–right. It was therefore impossible to assign an accurate fate for the wild-type ABxxx lineal homolog. These were **ABalp**ppa<u>l</u>aa and **ABalp**ppa<u>l</u>pa, which both made one muscle cell in *mex-3*, and **ABara**papa<u>l</u>, which made one hypodermal cell in *mex-3*. In wild-type embryos, **C**ppa produces 8 muscle cells and **C**papa produces 2 hypodermal cells. Hyp, hypodermal cells; mus, muscles; neur, neurons; death, programmed cell death.

single gene of unknown function that can encode a protein 83% identical to the predicted MEX-3 protein over the 131–amino acid region shown in Figure 5C. This human gene is therefore a candidate homolog of *mex-3*.

We found that the three missense mutations in *mex-3* all alter the second KH domain of the predicted MEX-3 protein (Figure 5D). The *mex-3(zu205)* and *mex-3(zu208)* mutations substitute Asp (G<u>A</u>A) and Arg (<u>A</u>GA), respectively, for Gly (GGA) at position 153, and *mex-3(or6)* substitutes Asp (G<u>A</u>A) for Gly (GGA) at position 156. The Gly residues altered by these mutations are in positions that are conserved in all KH domains described to date. Recent NMR structural analysis of a KH domain indicates that these Gly residues are part of an exposed flexible loop that may directly contact RNA (Musco et al., 1996).

mex-3 mRNA and Protein Are Distributed Asymmetrically in Early Embryos

We determined the localization of the *mex-3* gene products in hermaphrodite gonads and in early embryos. The localization of *mex-3* mRNA was determined by whole-mount in situ hybridization (Figure 6). The wild-type hermaphrodite gonad contains a linear array of developing germ cells and maturing oocytes (Figure 6B). *mex-3* mRNA is detected in the syncytial core of the distal gonad arm (Figure 6A) and is distributed uniformly in mature oocytes and in early 1-cell stage embryos (Figures 6A and 6C). However, in late 1-cell embryos *mex-3* mRNA is much more abundant in the anterior half of the embryo than in the posterior half (Figure 6D). After cytokinesis the anterior blastomere, AB, appears to have more *mex-3* mRNA than the posterior blastomere, P_1 (Figure 6E). In 4-cell stage embryos, both AB daughters have more *mex-3* mRNA than do the P_1 daughters (Figure 6F). After the 4-cell stage, *mex-3* mRNA disappears rapidly from the embryo in a pattern similar to that described previously for several unrelated maternal mRNAs in C. elegans. This pattern is thought to result from a general mechanism for RNA degradation in the soma and/or RNA stabilization in the germline lineage (Seydoux and Fire, 1994).

To examine the distribution of MEX-3 protein, we generated rabbit polyclonal and mouse monoclonal antibodies against full-length MEX-3 (see Experimental Procedures). All antisera result in identical staining patterns. In wild-type embryos, MEX-3 is present as a cytoplasmic protein that shows dynamic changes in its distribution

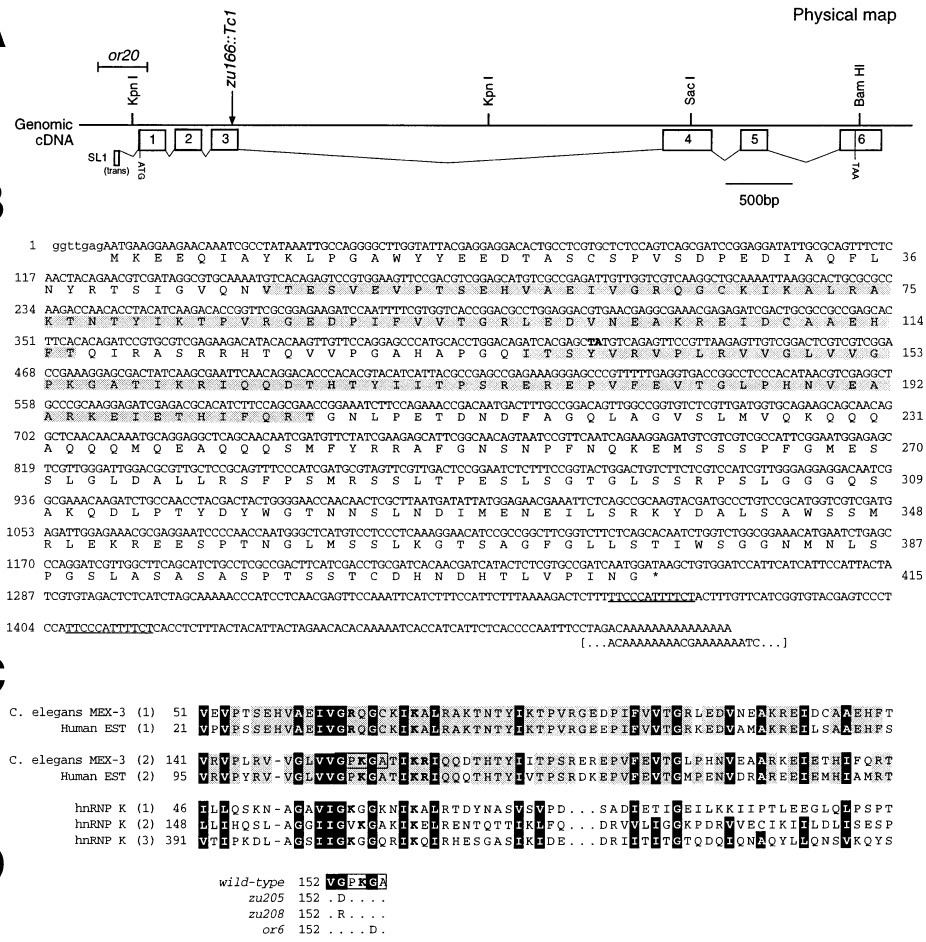

Figure 5. The *mex-3* Locus

(A) Physical map of the *mex-3* region showing molecular lesions described in the text.

(B) Nucleotide and predicted amino acid sequence of the *mex-3* cDNA. 5′ sequence corresponding to SL1 is shown in lower case letters. The *zu166::Tc1* transposon insertion is at position 426 (bold type). KH domains are shown shaded. The 3′UTR shown may not be complete because the end of the cDNA coincides with a genomic poly-A sequence (brackets). Direct repeats of unknown significance in the 3′UTR are underlined.

(C) KH domain sequences of MEX-3, a potential human homolog, and hnRNP K (Siomi et al., 1993). Highly conserved amino acids in all KH domain proteins are boxed in black (adapted from Siomi et al., 1994). The human sequence was determined by sequencing EST88186 (data not shown and Adams et al., personal communication).

(D) KH domain changes caused by three *mex-3* missense mutations.

among blastomeres during the early cleavage stages. These expression patterns are shown in Figure 7 and summarized in Figure 7G. MEX-3 protein is detected first in oocytes shortly after cellularization, and the amount of MEX-3 protein appears to increase in oocytes as they mature (Figure 7A). After fertilization, MEX-3 is distributed evenly throughout the cytoplasm of the 1-cell stage embryo (data not shown). By the end of the 2-cell stage, however, MEX-3 protein appears more abundant in the AB blastomere than in the P_1 blastomere (Figure 7B). In 4-cell stage embryos, MEX-3 appears more abundant in the AB daughters than in the P_1 daughters (Figure 7C). After the 4-cell stage, MEX-3 protein disappears from the embryo in a spatial and temporal pattern that is similar to the disappearance of *mex-3* mRNA (Figures 7D–7F).

MEX-3 Is a P Granule Component

In addition to the general cytoplasmic MEX-3 staining described above, we found that each of the MEX-3 antisera specifically stained distinct particles in P_1, and in the P_1 descendants P_2, P_3, and P_4 (for example, note the P_3 blastomere in Figure 7D). These particles are not detected in *mex-3* mutant embryos that lack MEX-3 (data not shown). The sizes and distributions of these particles are very similar to previously described structures called P granules (Strome and Wood, 1982). To determine the relationship between the MEX-3-containing particles and P granules, we stained early embryos simultaneously with an anti-MEX-3 antibody and an anti-P granule antibody. Confocal microscopy showed that the particles stained by the MEX-3 antisera coincide with P granules in the blastomeres P_1, P_2, P_3, and P_4 (Figures 8A and 8B and data not shown). However, the MEX-3 antisera do not stain P granules in the gonad (Figures 8C and 8D) or P granules in the germ cells of late stage embryos (data not shown). We conclude either that MEX-3 is a transient component of P granules only during the early cleavage stages, or that the MEX-3

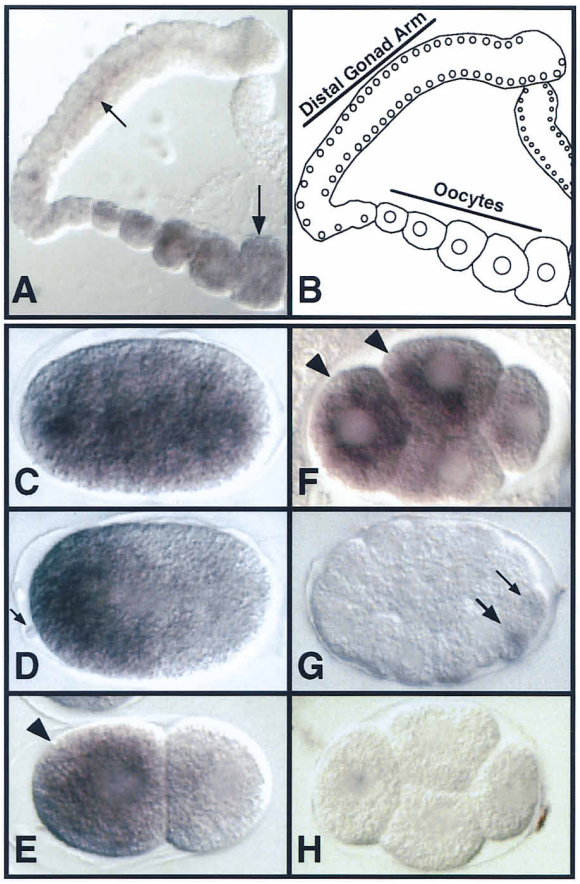

Figure 6. ***mex-3*** mRNA Is Distributed Asymmetrically in Early Embryos

Light micrographs of a wild-type hermaphrodite gonad (A) and early embryos (C–G) stained for *mex-3* mRNA by in situ hybridization (positive staining appears purple in photos).

(A) *mex-3* mRNA is detected in the syncytial core of the gonad (small arrow) and in mature oocytes (large arrow).

(B) Schematic diagram of (A). Open circles correspond to nuclei.

(C) Early 1-cell embryo.

(D) Late 1-cell embryo. Arrow points to polar body marking the anterior pole.

(E) 2-cell embryo. *mex-3* mRNA is more abundant in AB (arrowhead) than P_1.

(F) 4-cell embryo. Arrowheads point to the AB daughters.

(G) 28-cell embryo. *mex-3* mRNA, like many other maternal mRNAs, persists only in the germ cell precursor P_4 (large arrow) and its sister D (small arrow, see Seydoux and Fire, 1994).

(H) Wild-type 4-cell stage embryo hybridized with a *mex-3* sense RNA probe; compare with (F).

epitope is masked in P granules in the gonad and at later stages of embryogenesis.

Because MEX-3 protein associates with P granules in the early embryo, we asked if the distribution of P granules and the development of blastomeres that inherit them are affected in embryos that lack MEX-3. We found that the distribution of P granules was indistinguishable from wild-type embryos in 2- and 4-cell stage *mex-3* mutants (n = 46 and 49, respectively). However, in 16% of the 8-cell stage *mex-3* mutants examined, P granules were found in both P_3 and its sister C (13/83). In 76% of the 28-cell stage *mex-3* mutants examined, P granules were found in both daughters of P_3, the P_4 and D blastomeres (62/82). Although we have not detected defects in *mex-3* mutants in the development of the P_1 descendants MS, E, or C (Table 2), we have observed defects in the development of P_3. In *mex-3* mutant embryos, both daughters of P_3 often appear to produce several cells that morphologically resemble the germ cells normally produced only by the P_4 daughter (see Figure 2; Table 2 and data not shown). This result suggests that in some *mex-3* mutants, the D daughter is adopting the fate of P_4. Thus, in wild-type embryos, MEX-3 protein associates with P granules, appears to play a role in their proper segregation, and is required for the proper development of P_3, a blastomere that inherits them.

MEX-3 Negatively Regulates Muscle Development

We have shown that *mex-3* mutants have a major defect in the development of the anterior blastomere, AB, and a variable defect in one of the posterior descendants of P_1, the P_3 blastomere: the AB blastomere produces muscles inappropriately in *mex-3* mutants, and at least some P_3 blastomeres lose the ability to produce muscles. The expression pattern of MEX-3 is complex and is compatible with several models for MEX-3 function. It is possible that MEX-3 has distinct functions in AB and P_3, for example inhibiting muscle development in AB and inhibiting germ-cell development in certain P_3 descendants. Alternatively, MEX-3 could have a single function that is required for the proper development of both AB and P_3. For example, MEX-3 might function to localize an activator of muscle development to P_3. Because both models require some form of anterior–posterior asymmetry (i.e., the asymmetric localization of either an activator or repressor of muscle development), it should be possible to distinguish between them by analyzing muscle development in embryos that lack anterior–posterior asymmetry. If MEX-3 localizes a positive regulator, then mislocalization of this factor should cause AB and P_1 to produce muscles. Alternatively, if MEX-3 acts as a negative regulator of muscle development in AB, then mislocalization of MEX-3 activity might inhibit muscle production in both AB and P_1.

Mutations in the maternal gene *par-1* disrupt almost all of the known AB/P_1 asymmetries in the embryo. We found that MEX-3 was distributed equally between AB and P_1 at the 2-cell stage in *par-1* mutants (Figure 7H) and distributed equally between all blastomeres at the 4-cell stage (Figure 7I). We therefore asked whether AB and P_1 could produce muscles in a *par-1* mutant strain in which the SKN-1 contribution to muscle development was blocked by a mutation in the *skn-1* gene. We found that neither AB nor P_1 could produce muscles in most *skn-1;par-1* double mutants (Figures 3G and 3H) (see also Bowerman et al., 1993). To determine if *mex-3(+)* activity was preventing muscle development in the double mutant, we constructed and analyzed *mex-3;skn-1;par-1* mutant embryos. In these triple mutant embryos, we found that both AB and P_1 produced numerous muscles (Figures 3I and 3J; Table 1). This result indicates that *mex-3(+)* activity prevents the development of muscle in *skn-1;par-1* double mutant embryos and is consistent with the hypothesis that MEX-3 functions in wild-type AB blastomeres to prevent muscle development.

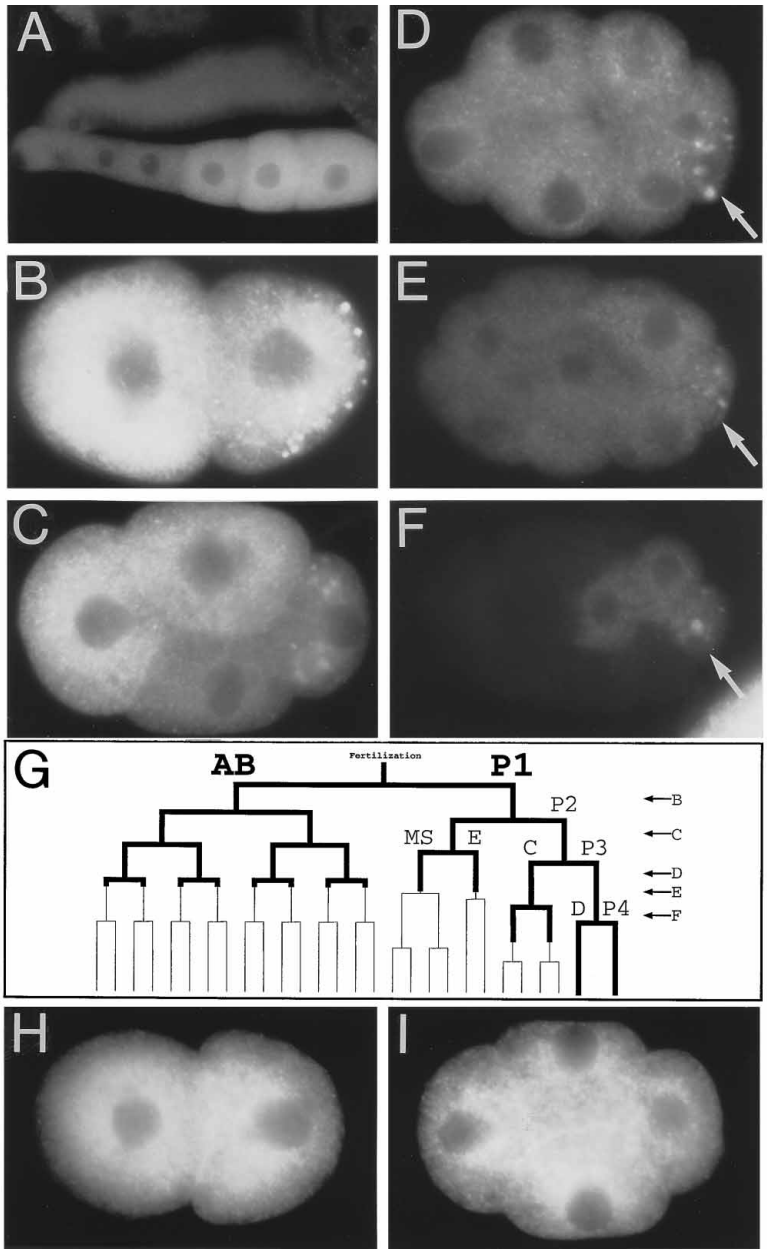

Figure 7. Distribution of MEX-3 Protein

Immunofluorescence micrographs of a wild-type hermaphrodite gonad (A) and early embryos stained for MEX-3 protein with monoclonal antibody D45D2.

(A) Low magnification image of a hermaphrodite gonad oriented as in Figure 6A. (B–F) High magnification pictures of early embryos oriented as diagrammed in Figure 1; all photos are equivalent exposures. (B) 2-cell embryo. Note granules in P_1 cytoplasm. (C) 4-cell embryo. During the 8-cell (D), 12-cell (E), and 15-cell (F) stages MEX-3 disappears from all AB descendants but persists transiently in P_1 descendants; arrow points to the P_3 blastomere. (G) Summary of MEX-3 distribution. Lineage diagram to the 28-cell stage of embryogenesis is shown. Bold lines indicate presence of MEX-3 protein. Letters at right correspond to panels shown above. In 2-cell (H) and 4-cell (I) *par-1(e2012)* embryo, MEX-3 is present at similar levels in all blastomeres.

Discussion

After the first division of the fertilized egg, the sister blastomeres AB and P_1 have intrinsic differences in their abilities to produce muscles; P_1 can produce muscles but AB cannot (Laufer et al., 1980; Cowan and McIntosh, 1985; Priess and Thomson, 1987). The unequal distribution of the SKN-1 protein appears to account for part, but not all, of this asymmetry (Mello et al., 1992; Bowerman et al., 1993). In this paper we have provided evidence that MEX-3 has a role in AB/P_1 asymmetry that is independent of SKN-1 localization or activity. We have shown that MEX-3 contains probable RNA-binding motifs, suggesting that MEX-3 may regulate the expression of one or more RNAs in the early embryo. In the accompanying manuscript, Hunter and Kenyon (1996 [this issue of *Cell*]) show that the homeodomain protein PAL-1, the C. elegans homolog of Drosophila CAUDAL (Waring and Kenyon, 1991), is expressed inappropriately in AB descendants in *mex-3* mutants, suggesting that at least part of MEX-3's function is to regulate the *pal-1* mRNA.

Muscle Development in C. elegans Embryos

In wild-type development, three of the four P_1 granddaughters produce muscles (see Figure 1). The MS granddaughter of P_1 produces primarily muscles and pharyngeal cells, the C granddaughter produces muscles and hypodermal cells, and the P_3 granddaughter produces muscles and germ cells (Sulston et al., 1983). Previous studies had suggested that the P_1 granddaughters must acquire the ability to produce muscles through

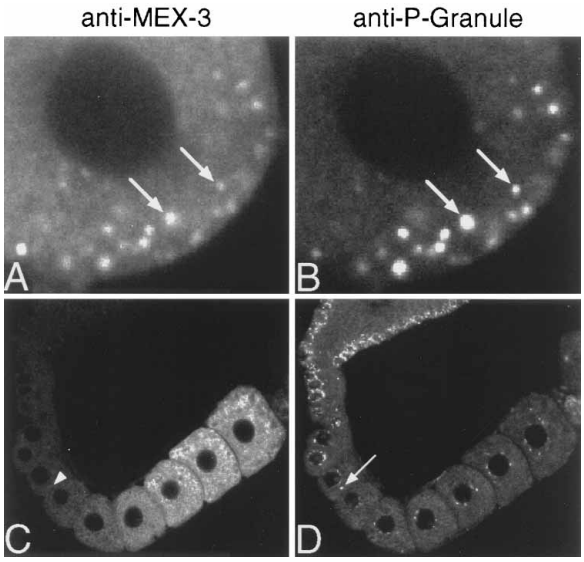

Figure 8. MEX-3 and P Granules

(A and B) Confocal immunofluorescence micrographs of a wild-type P_1 blastomere double stained with antibodies against MEX-3 (A) and against P granules (B). Arrows point to two of the granules recognized by both antisera.

(C and D) Immunofluorescence micrographs of a hermaphrodite gonad double stained for MEX-3 (C) and P granules (D). Arrowhead in (C) shows the absence of staining at the position of a P granule in (D) (arrow).

different genetic pathways (Mello et al., 1992; Bowerman et al., 1993; Schnabel, 1994). However, the only genes that had been implicated in muscle development all appeared to play a role in specifying the fate of the MS blastomere. For example, several mutants have been identified that cause AB descendants to develop with characteristics of a wild-type MS blastomere, apparently due to the inappropriate expression of SKN-1 in AB (Mello et al., 1992; Bowerman et al., 1993; Schnabel et al., 1996). These studies have suggested that SKN-1 plays a role in specifying the MS pattern of development, but that SKN-1 is not involved in specifying the C or P_3 patterns. Similarly, the GLP-1 protein, which is related to Drosophila NOTCH, and the POP-1 protein, which is related to lymphoid-specific transcriptional regulators in vertebrates, have been shown to be required for MS, but not for C or P_3, to produce muscles (Schnabel, 1994; Lin et al., 1995).

We have shown here that mutations in *mex-3* cause AB descendants to develop with characteristics of a wild-type C blastomere. This observation suggests that wild-type embryos contain a factor(s) that specifies the C fate and that *mex-3(+)* prevents this factor from functioning in AB or AB descendants. These AB descendants that adopt the C-like fate are born about the same time as the C blastomere itself is born (see Figure 7G). This result suggests that there is a limited time in embryogenesis when the C fate can be specified or expressed and that *mex-3* mutations do not effect the timing of this event. Thus *mex-3(+)* appears to function in determining the spatial, but not temporal, expression of the C fate in wild-type embryos.

MEX-3 and the Regulation of Maternal mRNAs

Our molecular analysis of *mex-3* indicates that the MEX-3 protein contains two probable RNA-binding motifs, called KH domains. Cross-linking studies have demonstrated direct interactions between RNA and the KH motifs found in the ribosomal protein S3 (Urlaub et al., 1995), and in the Escherichia coli protein NusA (Liu and Hanna, 1995). Mutational analysis has demonstrated that the KH domains in the vertebrate proteins hnRNP K and FMR1 are essential for RNA binding in vitro (Siomi et al., 1994). We have shown that missense mutations that alter invariant residues in the KH domains of MEX-3 cause phenotypes indistinguishable from mutations that prevent expression of MEX-3 altogether. It is therefore likely that MEX-3 regulates C development by regulating RNA expression, localization, or metabolism.

We have used *par-1* mutant embryos to examine possible MEX-3 functions. The AB and P_1 blastomeres in *par-1* mutants appear to have nearly symmetrical patterns of development and have identical expression patterns of almost all molecular markers reported thus far, including MEX-3 itself (Kemphues et al., 1988; Kirby et al., 1990; Bowerman et al., 1993; Guo and Kemphues, 1995; this work). If MEX-3 localizes posteriorly an mRNA required for C development, we would anticipate that this mRNA would not be localized in *par-1* mutants. This model predicts that AB and P_1 should both produce C-like muscles in *par-1;skn-1* mutants independent of *mex-3* function. Instead, we found that neither AB nor P_1 could produce such muscles in most *par-1;skn-1* mutants when MEX-3 was present. We thus propose that MEX-3 functions in generating muscle asymmetry by repressing, in AB descendants, the expression of an mRNA(s) that normally specifies the C pattern of development.

If MEX-3 inhibits a C pattern of development in AB descendants, but not in P_1, what controls the AB/P_1 asymmetry of MEX-3 function? It is possible that the activity of MEX-3 is regulated by asymmetrically localized factors such as the P_1-specific kinase PAR-1 (Guo and Kemphues, 1995). Alternatively, we have observed two AB/P_1 asymmetries in the distribution of MEX-3 itself that could result in an asymmetry in MEX-3 activity. First, MEX-3 appears to be present at higher levels in AB and the AB daughters, than in P_1 or the P_1 daughters. Second, a large amount of MEX-3 protein in P_1, and in P_1 descendants, is localized to P granules. As the molecular mechanisms of protein localization become better understood, it should be possible to alter the expression patterns of MEX-3 to test whether these asymmetries are functionally significant.

MEX-3 and PAL-1

C. elegans embryos control the expression of maternal mRNAs both temporally and spatially (Bowerman et al., 1993; Evans et al., 1994; Seydoux and Fire, 1994; Lin et al., 1995; Hunter and Kenyon, 1996; Mello et al., 1996; Mickey et al., 1996). The genes *pop-1, skn-1, pie-1, glp-1, apx-1, pal-1,* and *mex-3* are all transcribed in the maternal gonad. Although the POP-1 and MEX-3 proteins are detected easily in oocytes, the protein products of the other messages are not detected until various

times after fertilization and cleavage. With the exception of the *mex-3* mRNA, each of these mRNAs appears to be distributed equally between AB and P_1. However, GLP-1 protein is present exclusively in AB descendants, while the proteins SKN-1, PIE-1, APX-1, and PAL-1 are present exclusively or predominately in P_1 descendants (Bowerman et al., 1993; Evans et al., 1994; Hunter and Kenyon, 1996; Mello et al., 1996; Mickey et al., 1996). Although factors that specify these expression patterns have not yet been identified, two cis-acting elements in the 3′ UTR of the *glp-1* mRNA have been shown to be required for proper temporal and spatial expression; one element appears to prevent translation of the *glp-1* mRNA in oocytes, and the second prevents expression in P_1 descendants (Evans et al., 1994).

KH domains have not yet been demonstrated to bind RNA with sequence specificity. However, MEX-3 cannot be a general regulator of maternal mRNA expression because SKN-1, GLP-1, and APX-1 each have normal temporal and spatial expression patterns in *mex-3* mutant embryos. MEX-3 may regulate *pal-1* mRNA expression, however, because the PAL-1 protein is expressed inappropriately in *mex-3* mutants (Hunter and Kenyon, 1996). In wild-type oocytes, MEX-3 is present at high levels (this work) and PAL-1 is not detectable (Hunter and Kenyon, 1996). In *mex-3* mutant oocytes, MEX-3 is not present and PAL-1 is expressed at high levels. In wild-type 4-cell embryos, both *mex-3* mRNA and MEX-3 protein are present at higher levels in AB descendants than in P_1 descendants, and PAL-1 is expressed only in P_1 descendants. In *mex-3* mutant 4-cell embryos, PAL-1 is expressed in each AB and P_1 descendant (Hunter and Kenyon, 1996). Thus in wild-type development, the primary role of MEX-3 could be to prevent PAL-1 expression in oocytes. Alternatively, MEX-3 could be required continuously during the early cleavage stages to prevent PAL-1 expression in AB descendants.

Eliminating or reducing maternal *pal-1(+)* activity can prevent both C and P_3 from producing muscles (Hunter and Kenyon, 1996). Although PAL-1 is expressed inappropriately in AB descendants in *mex-3* mutants, we have shown that these descendants appear to adopt C-like fates. It is possible that PAL-1 is sufficient to specify the C pattern of development but functions together with other factors to specify the P_3 pattern. Consistent with this hypothesis, maternal *pie-1(+)* activity is known to be required for the proper development of one of the P_3 daughters (Mello et al., 1992), and the PIE-1 protein has been shown recently to be present in P_3 but not C (Mello et al., 1996). Thus SKN-1, PAL-1, and PIE-1 play major roles in permitting the MS, C, and P_3 patterns of development, and there appear to be separate mechanisms that determine which blastomeres express these factors.

MEX-3 and P Granules

P granules were defined immunologically in C. elegans by several different antibodies, such as K76, that showed identical staining patterns of P granules in gonads, oocytes, and embryos (Strome and Wood, 1982). During embryonic development, the P granules are partitioned specifically into the germline precursors and appear to contain mRNAs of unknown identity (Strome and Wood, 1982; Seydoux and Fire, 1994). Interestingly, MEX-3 can be detected in P granules only in early cleavage stage embryos, suggesting that the composition of P granules changes during early development. Because MEX-3 is likely to be an RNA-binding protein, its association with P granules may provide a method for localizing certain RNAs to the germline precursors. During the period that MEX-3 protein disappears from AB descendants, P granules containing MEX-3 are concentrated into the P_3 blastomere. RNA(s) essential for P_3 development might thus be brought into P_3 through association with MEX-3.

We have found that *mex-3* mutations cause defects in the development of the P_3 blastomere in addition to the defects observed in AB development. The P_3 defect in *mex-3* mutants does not result from the aberrant development of the AB descendants, because this defect persists even after the AB blastomere is killed. Injecting antisense *pal-1* RNA into *mex-3* mutants can suppress the AB defect but does not appear to suppress the P_3 defect (Hunter and Kenyon, 1996). These results suggest that MEX-3 may have separate functions in AB and P_3 development. Thus MEX-3 appears to be required for the proper regulation of *pal-1* mRNA but to have at least one additional function required for P_3 development, perhaps related to its association with P granules.

In conclusion, the asymmetrically distributed PAR proteins at the cortex of the C. elegans embryo must somehow determine the asymmetric expression of proteins like PAL-1 and SKN-1 that regulate gene expression. MEX-3 provides a possible link between these two classes of proteins, though much remains to be learned about how this occurs. The observations that MEX-3 (this report) and PAL-1 (Waring and Kenyon, 1991) both appear to be highly conserved in animals suggests the interesting possibility that regulatory interactions between these proteins may have persisted in animal evolution.

Experimental Procedures

Strains and Alleles

The Bristol strain N2 was used as the standard wild-type strain. The marker mutations, deficiencies, and balancer chromosomes used are listed by chromosome as follows: LG*I*: *bli-3(e767), dpy-5(e61), egl-30(ad805), mex-3*(*or6, or20, or30, zu142, zu155, zu166::Tc1, zu171, zu176::Tc1, zu181, zu205, zu208, zu211*, and *zu219*), *spe-8(hc40), spe-13(hc137), hDf10, hT1(I;IV), hT2(I;III)*; LG*II*: *bli-2(e768)*; LG*IV*: *dpy-13(e184), skn-1(zu67); unc-5(e53), unc-8(n491), DnT1 (IV;V)*; LG*V*: *dpy-11(e224), him-5(e1409) par-1(e2012), rol-4(sc8)*; LG*X*: *lin-2(e1309), lon-2(e678)*. The *mex-3*(*or6, or20*, and *or30*) mutations were isolated by Chris Thorpe and Paula Martin. *mex-3(zu203, zu205, zu211*, and *zu219*) were isolated by Rueyling Lin. The deficiency *hDf10* was provided by Ann Rose. All other mutant alleles were obtained, or are available, from the C. elegans Genetic Center, which is funded by the NIH National Center for Research Resources (NCRR). The basic methods of C. elegans culture, mutagenesis, and genetics were as described in Brenner (1974).

Isolation of *mex-3* Alleles

The *mex-3* alleles *zu142, zu155, zu203, zu205, zu211, zu219, or6, or20*, and *or30* were isolated by a screening method described in Priess et al. (1987), and *zu166::Tc1, zu171, zu76::Tc1*, and *zu181* were isolated in a screen described in Mello et al. (1994). All alleles failed to complement *mex-3(zu155)*.

Genetic Analysis

mex-3(zu155) was mapped to the left arm of LGI, near *spe-8*, using standard two- and three-factor genetic analysis. Map data is available from the C. elegans Genetic Center. The deficiency hDf10 fails to complement *mex-3(zu155)*, as shown by the following test: *mex-3(zu155)dpy-5(e61)/hT1; him-5(e1491)* males were mated to hDf10 *dpy-5(e61)/hT2* hermaphrodites. All (8/8) Dpy F1 hermaphrodite progeny developed to adults and produced all dead progeny; these embryos arrested development with phenotypes indistinguishable from embryos produced by mothers homozygous for *mex-3 (zu155)* (data not shown). The alleles used in this study to characterize the mutant phenotype were backcrossed at least eight times to the parental N2 strain. The *mex-3* gene is required maternally as shown by the following test. No viable self-progeny were produced by hermaphrodites homozygous for *mex-3(zu155)egl-30(ad805)* (0%; n > 10,000). No viable cross progeny were obtained after purged hermaphrodites homozygous for *mex-3(zu155)* were mated to wild-type males (0%; n = 386). *mex-3* is not required zygotically, as shown by the following analysis with the null allele *mex-3(or20)*: all embryos produced by a *mex-3(or20)egl-30(ad805)/++* hermaphrodite are viable (100%, n = 1896).

Molecular Analysis of *mex-3*

The genomic DNA flanking a Tc1 element associated with the *mex-3(zu166::Tc1)* mutation was cloned as described in Hill and Sternberg (1992). cDNA clones were isolated from a mixed stage cDNA library provided by Andy Fire. Reverse transcription and the polymerase chain reaction were used to detect *mex-3* RNA transpliced to SL1 using conditions described in Spieth et al. (1993).

In Situ Hybridization

The in situ hybridization protocol was as described in Seydoux and Fire (1994). No staining was detected with sense probe in wild-type embryos (see Figure 6H), and no staining was detected with antisense probe in *mex-3(zu155)* mutant embryos (B. D., unpublished data).

Production of Antibodies and Immunostaining

Rabbits and mice were immunized with either full-length MEX-3 (MEX-$3^{1–415}$), or the COOH-terminal 187 amino acids of MEX-3 (MEX-$3^{253–415}$) expressed using the pET-16b vector (Novagen). Monoclonal antibodies D45D2 and H47C4 were generated as described by Harlow and Lane (1988). Identical staining patterns were obtained from each polyclonal antisera and monoclonal cell supernatant. Fixation and immunostaining of embryos was as described in Albertson (1984).

For double immunofluorescence of MEX-3 and P-granules, fixed gonads and embryos were stained simultaneously with a 1:100 dilution of anti-MEX-$3^{1–415}$ rabbit polyclonal sera, and undiluted anti-P-granule mouse monoclonal antibody K76. Following washes, specimens were incubated simultaneously with rhodamine-conjugated goat-anti-mouse and fluorescein-conjugated donkey-anti-rabbit immunoglobulin G antibodies (TAGO). The fluorochrome-conjugated goat-anti-mouse and donkey-anti-rabbit antibodies were tested and shown not to cross-react. Slides were examined by laser scanning confocal microscopy on a Bio-Rad MRC600 LSCM (Bio-Rad Microscope Division, Cambridge, Massachusetts).

Microscopy

Laser ablation experiments were performed as previously described (Bowerman et al., 1992; Mello et al., 1992). Details of laser ablation experiments are given below. The identity of differentiated cells in experimental embryos were assigned based on morphological criteria in the light microscope, followed in most cases by analysis with tissue-specific probes: pharyngeal tissue was scored by mAb 3NB12 (Priess and Thomson, 1987), muscle with mAb 5.6 (Miller et al., 1983), and neurons with anti-UNC-33 (W. Li et al., personal communication). Criteria for assigning body-wall muscle cell, intestinal cell, pharyngeal cell, and hypodermal cell fates were as previously described (Bowerman et al., 1992; Mello et al., 1992). In Figure 2 and Table 1, the ability of the AB or P_1 blastomere to produce muscle was assessed by killing the other blastomere with a laser microbeam shortly following the division of P_0. For Table 1 the following procedures were used to assess the ability of AB to produce specific tissues: pharyngeal production was as described in Hutter and Schnabel (1994), neural production was determined by killing P_1 at the 2-cell stage, and intestinal valve cells formation was as described in Mango et al. (1994). For Table 2, ABal development was determined by killing ABp, EMS, and P_2 in 4-cell stage embryos with a laser microbeam, and killing ABar immediately after the division of ABa. All other AB granddaughters were analyzed in analogous experiments.

Lineage Analysis

Lineage analysis was performed from video images using a Nikon Optiphot II microscope equipped with differential interference contrast optics and a Z-axis electronic focus operated with a Ludl Mac2000 controlled by a Power Macintosh 8100 computer equipped with a Scion LG3 8 bit frame grabber. Device control and image acquisition are accomplished using a modified version of NIH Image. In typical experiments, 25–30 focal planes spaced 0.5 μm apart were collected at 30 s intervals for 7–8 hr. Images were acquired uncompressed, and then compressed and compiled into a QuickTime movie. NIH Image is a public domain software program written by Wayne Rasband and is available by anonymous ftp from ftp.zippy.nimh.nih.gov. 4D software is available upon request by contacting J. H. at hardin@macc.wisc.edu. The lineage data presented in Figure 4 and Table 3 were obtained from analyzing 4D recordings of two *mex-3(zu155)* mutant embryo.

Acknowledgments

The authors thank the laboratories of J. Shaw and J. Kimble for providing antibodies; C. Hunter, C. Kenyon, K. Mickey and J. Shaw for communicating unpublished data; and M. Costa, R. Hill, C. Goutte, and D. Waring for critical comments on this manuscript. We are indebted to C. Thorpe, P. Martin, and R. Lin for providing additional *mex-3* alleles; K. Neugebauer and M. Roth for their advice and assistance in generating hybridoma cell lines. Some strains used in this work were provided by the C. elegans Genetic Toolkit Project, funded by an NIH National Center for Research Resources grant to A. Rose, D. Baillie, and D. Riddle. The authors wish to dedicate this paper to the memory of Hal Weintraub, a great friend and a remarkable colleague. Hal's support, advice, encouragement, and humor not only made this work possible, but also a great deal of fun. B. W. D., and C. C. M. were supported by grants from the NIH, B. B. by the Jane Coffin Childs Medical Research Fund, and J. H. by a Scholar Award in the Biomedical Sciences from the Lucille P. Markey Charitable Trust, NSF Young Investigator Award, and the NIH. J. R. P. is supported by the Howard Hughes Medical Institute.

Received June 4, 1996; revised September 6, 1996.

References

Albertson, D.G. (1984). Formation of the first cleavage spindle in nematode embryos. Dev. Biol. *101*, 61–72.

Ashley, C.T., Jr., Wilkinson, K.D., Reines, D., and Warren, S.T. (1993). FMR1 protein: conserved RNP family domains and selective RNA binding. Science *262*, 563–566.

Blackwell, T.K., Bowerman, B., Priess, J.R., and Weintraub, H. (1994). Formation of a monomeric DNA binding domain by Skn-1 bZIP and homeodomain elements. Science *266*, 621–628.

Bowerman, B., Eaton, B.A., and Priess, J.R. (1992). *skn-1*, a maternally expressed gene required to specify the fate of ventral blastomeres in the early C. elegans embryo. Cell *68*, 1061–1075.

Bowerman, B., Draper, B.W., Mello, C.M., and Priess, J.R. (1993). The maternal gene *skn-1* encodes a protein that is distributed unequally in early C. elegans embryos. Cell *74*, 443–452.

Brenner, S. (1974). The genetics of Caenorhabditis elegans. Genetics *77*, 71–94.

Cheng, N.N., Kirby, C.M., and Kemphues, K.J. (1995). Control of cleavage spindle orientation in Caenorhabditis elegans: the role of the genes par-2 and par-3. Genetics *139*, 549–559.

Cowan, A.E., and McIntosh, J.R. (1985). Mapping the distribution of differentiation potential for intestine, muscle, and hypodermis during early development in Caenorhabditis elegans. Cell *41*, 923–932.

Etemad-Moghadam, B., Guo, S., and Kemphues, K.J. (1995). Asymmetric distribution of PAR-3 protein contributes to cell polarity and spindle alignment in early C. elegans embryos. Cell *83*, 743–752.

Evans, T.C., Crittenden, S.L., Kodoyianni, V., and Kimble, J. (1994). Translational control of maternal *glp-1* mRNA establishes an asymmetry in the C. elegans embryo. Cell *77*, 183–194.

Gibson, T.J., Rice, P.M., Thompson, J.D., and Heringa, J. (1993). KH domains within the FMR1 sequence suggest that fragile X syndrome stems from a defect in RNA metabolism. Trends Biochem. Sci. *18*, 331–333.

Guo, S., and Kemphues, K.J. (1995). *par-1*, a gene required for establishing polarity in C. elegans embryos, encodes a putative Ser/Thr kinase that is asymmetrically distributed. Cell *81*, 611–620.

Harlow, E., and Lane, D. (1988). Antibodies: A Laboratory Manual (Cold Spring Harbor, New York: Cold Spring Harbor Laboratory).

Hill, R., and Sternberg, P. (1992). The gene *lin-3* encodes an inductive signal for vulval development in C. elegans. Nature *358*, 470–476.

Hunter, C.P., and Kenyon, C. (1996). Spatial and temporal controls target *pal-1* blastomere-specification activity to a single blastomere lineage in C. elegans embryos. Cell, this issue.

Hutter, H., and Schnabel, R. (1994). *glp-1* and inductions establishing embryonic axis in Caenorhabditis elegans. Development *120*, 2051–2064.

Ito, K., Sato, K., and Endo, H. (1994). Clonal characterization of a single-stranded DNA binding protein that specifically recognizes deoxycytidine stretch. Nucleic Acids Res. *22*, 53–58.

Jones, A.R., and Schedl, T. (1995). Mutations in *gld-1*, a female germ cell–specific tumor suppressor gene in Caenorhabditis elegans, affects a conserved domain also found in Src-associated protein Sam68. Genes Dev. *9*, 1491–1504.

Kemphues, K.J., Priess, J.R., Morton, D.G., and Cheng, N. (1988). Identification of genes required for cytoplasmic localization in early C. elegans embryos. Cell *52*, 311–320.

Kirby, C., Kusch, M., and Kemphues, K. (1990). Mutations in the *par* genes of Caenorhabditis elegans affect cytoplasmic reorganization during the first cell cycle. Dev. Biol. *142*, 203–215.

Krause, M., and Hirsh, D. (1987). A trans-spliced leader sequence on actin mRNA in C. elegans. Cell *49*, 753–761.

Laufer, J.S., Bazzicalupo, P., and Wood, W.B. (1980). Segregation of developmental potential in early embryos of Caenorhabditis elegans. Cell *19*, 569–577.

Leffers, H., Dejgaard, K., and Celis, J.E. (1995). Characterization of two major cellular poly(rC)-binding human proteins each containing three K-homology (KH) domains. Eur. J. Biochem. *230*, 447–453.

Lin, R., Thompson, S., and Priess, J.R. (1995). *pop-1* encodes an HMG box protein required for specification of a mesodermal precursor in early C. elegans embryos. Cell *83*, 599–609.

Liu, K., and Hanna, M.M. (1995). NusA contacts nascent RNA in Escherichia coli transcription complexes. J. Mol. Biol. *247*, 547–558.

Mahone, M., Saffman, E.E., and Lasko, P.F. (1995). Localized *Bicaudal-C* RNA encodes a protein containing a KH domain, the RNA binding motif of FMR1. EMBO J. *14*, 2043–2055.

Mango, S.E., Thorpe, C.J., Martin, P.R., Chamberlain, S.H., and Bowerman, B. (1994). Two maternal genes, *apx-1* and *pie-1*, are required to distinguish the fates of equivalent blastomeres in the early Caenorhabditis elegans embryo. Development *120*, 2305–2315.

Mello, C.C., Draper, B.W., Krause, M., Weintraub, H., and Priess, J.R. (1992). The *pie-1* and *mex-1* genes and maternal control of blastomere identity in early C. elegans embryos. Cell *70*, 163–176.

Mello, C.C., Schubert, C., Draper, B., Zhang, W., Lobel, B., and Priess, J.R. (1996). The PIE-1 protein and germline specification in early C. elegans embryos. Nature *382*, 710–712.

Mickey, K.M., Mello, C.C., Montgomery, M.K., Fire, A., and Priess, J.R. (1996). An inductive interaction in 4-cell stage C. elegans embryos involves APX-1 expression in the signaling cell. Development *122*, 1791–1798.

Miller, D.M., III, Oritz, I., Berliner, G.C., and Epstein, H.F. (1983). Differential localization of two myosins within nematode thick filaments. Cell *34*, 477–490.

Mori, I., Moerman, G., and Waterston, R.H. (1988). Analysis of a mutator activity necessary for germline transposition and excision of Tc1 transposable elements in Caenorhabditis elegans. Genetics *120*, 397–407.

Morton, D.G., Roos, J.M., and Kemphues, K.J. (1992). *par-4*, a gene required for cytoplasmic localization and determination of specific cell types in Caenorhabditis elegans embryogenesis. Genetics *130*, 771–790.

Musco, G., Stier, G., Joseph, C., Morelli, M.A.C., Nilges, M., Gibson, T., and Pastore, A. (1996). Three-dimensional structure and stability of the KH domain: molecular insights into the Fragile X syndrome. Cell *85*, 237–245.

Priess, J.R., and Thomson, J.N. (1987). Cellular interactions in early C. elegans embryos. Cell *48*, 241–250.

Schnabel, R. (1994). Autonomous and nonautonomy in cell fate specification of muscle in the C. elegans embryo: a reciprocal induction. Science *263*, 1449–1452.

Schnabel, R. (1996). Pattern formation: regional specification in the early C. elegans embryo. Bioessays *18*, 591–594.

Schnabel, R., Weigner, C., Hutter, H., Feichtinger, R., and Schnabel, H. (1996). *mex-1* and the general partitioning of cell fate in the early C. elegans embryo. Mech. Dev. *54*, 133–147.

Seydoux, G., and Fire, A. (1994). Soma-germline asymmetry in the distribution of embryonic RNAs in Caenorhabditis elegans. Development *120*, 2823–2834.

Siomi, H., Matunis, M.J., Michael, W.M., and Dreyfuss, G. (1993). The pre-mRNA binding K protein contains a novel evolutionarily conserved motif. Nucleic Acids Res. *21*, 1193–1198.

Siomi, H., Choi, M., Siomi, M.C., Nussbaum., R.L., and Dreyfuss, G. (1994). Essential role for KH domains in RNA binding: impaired RNA binding by mutations in the KH domain of FMR1 that causes fragile X syndrome. Cell *77*, 33–39.

Spieth, J., Brooke, G., Kuersten, S., Lea, K., and Blumenthal, T. (1993). Operons in C. elegans: polycistronic mRNA precursors are processed by trans-splicing of SL2 to downstream coding regions. Cell *73*, 521–532.

Strome, S., and Wood, W.B. (1982). Immunofluorescence visualization of germ-line-specific cytoplasmic granules in embryos, larvae, and adults of Caenorhabditis elegans. Proc. Natl. Acad. Sci. *79*, 1558–1562.

Sulston, J.E., Schierenberg, E., White, J.G., and Thomson, J.N. (1983). The embryonic cell lineage of the nematode Caenorhabditis elegans. Dev. Biol. *100*, 64–119.

Urlaub, H., Kruft, V., Bischof, O., Mueller, E.C., and Whittman-Liebold, B. (1995). Protein-rRNA binding features and their structural and functional implications in ribosomes as determined by cross-linking studies. EMBO J. *14*, 4578–4588.

Waring, D.A., and Kenyon, C. (1991). Regulation of cellular responsiveness to inductive signals in the developing C. elegans nervous system. Nature *350*, 712–715.

GenBank Accession Number

The accession number for the sequence reported in this paper is U67864.